JOURNAL OF GEOPHYSICAL RESEARCH, VOL. 115, F01012, doi:10.1029/2009JF001261, 2010

Wind influence on snow depth distribution and accumulation over glaciers

R. Dadic,[1,2] R. Mott,[3] M. Lehning,[3] and P. Burlando[1]

Received 13 January 2009; revised 4 September 2009; accepted 23 October 2009; published 18 March 2010.

[1] In mountain regions wind is known to cause snow redistribution. While physically based models of snow redistribution have been developed for flat to gently rolling terrain, extension of these findings to steep terrain has been limited by the complexity of wind fields in such areas. In this study, we applied a nonhydrostatic and compressible atmospheric prediction model to steep alpine topography and compared the results to a fully distributed data set of snow depth estimations. The results show reduced horizontal wind velocity as well as an increasing downward vertical wind velocity over areas with the largest winter accumulation, which are mostly glacierized. We show that the wind velocity normal to the local surface, which should be zero in a nondivergent flow field and is a direct measure of increased or decreased local deposition, is a function of small-scale features of local topography. The correlation between wind fields, snow accumulation, and glacierization suggests that accurate modeling of wind fields over glacierized areas in complex terrain is a key factor for understanding the mass balance distribution of glaciers.

Citation: Dadic, R., R. Mott, M. Lehning, and P. Burlando (2010), Wind influence on snow depth distribution and accumulation over glaciers, *J. Geophys. Res.*, *115*, F01012, doi:10.1029/2009JF001261.

1. Introduction

[2] In mountain regions wind is known to cause snow redistribution. Local winds also influence the energy exchange and mass exchange over snow, strongly affecting snow and ice melt and hence the glacier mass balance [e.g., *Gray and Male*, 1981; *Winstral and Marks*, 2002]. *Machguth et al.* [2006], using airborne ground penetrating radar (GPR), observed a high variability of winter snow distribution along centerlines of two adjacent alpine glaciers, and they suggest that this variability was primarily caused by wind-driven processes and, on a larger scale, by horizontal precipitation gradients.

[3] While the daily ablation rate of ice that is fully exposed to the Sun may be twice that of ice in the shade, wind-driven processes and avalanches may locally multiply winter accumulation by a large factor [*Kuhn*, 1995]. Especially for small cirque glaciers, which occur in bowl-shaped depressions on the side of mountains, unevenly distributed precipitation and snow transport, along with avalanches, are governing factors for their sustainment [*Kuhn*, 1995, 2003; *Hoffmann et al.*, 2007]. The occurrence of small cirque glaciers at all aspects agrees with the general assumption that the mass balance of small glaciers is dominated more by winter accumulation and less by the energy balance [*Kuhn*, 1995; *Hoffmann et al.*, 2007]; hence, the importance of the processes that lead to snow accumulation must be investigated.

[4] Physically based, spatially distributed models of snow redistribution have been developed for flat to gently rolling terrain [e.g., *Pomeroy et al.*, 1993; *Liston and Sturm*, 1998], but extensions of these findings to steep terrain as found in the Alps or the Himalayas have been limited by the complexity of wind fields in such areas [*Liston and Sturm*, 1998; *Winstral et al.*, 2002] because the boundary layer flow over steep terrain is highly turbulent and is therefore nonlinear because of local pressure-terrain interactions [*Raderschall et al.*, 2008]. Snow distribution by wind can be caused by different processes. One of these processes is snow drift, where the increase of wind speed in the windward side of ridges increases erosion, while the decrease in wind speed in the lee of ridges increases deposition [e.g., *Mellor*, 1965; *Radok*, 1977; *Pomeroy*, 1988; *Liston and Sturm*, 1998; *Clifton and Lehning*, 2008]. Another process occurs when reduced wind velocity leeward of the ridges results in increased precipitation and additional snow deposition [*Föhn and Meister*, 1983; *Gauer*, 2001; *Mott et al.*, 2008]. *Lehning et al.* [2008] explained this process with higher wind velocities and updrafts, which cause reduced deposition velocities for snow during precipitation in the windward side of a mountain ridge, while the deposition velocities are increased through lower wind speeds in the lee of a ridge. They introduce the term "preferential deposition" in this context as a process mainly governed by winds and not dependent on ground snow surface properties, as it is in the case of erosion and deposition of already deposited snow, known as

[1] Institute of Environmental Engineering, ETH Zurich, Zurich, Switzerland.
[2] Department of Atmospheric Sciences, University of Washington, Seattle, Washington, USA.
[3] WSL Institute for Snow and Avalanche Research SLF, Davos, Switzerland.

0148-0227/10/2009JF001261

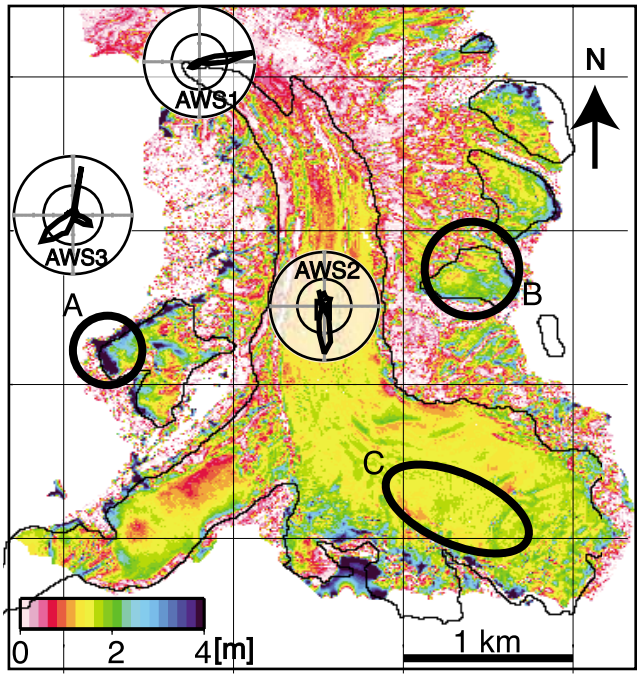

Figure 1. Snow depth distribution (m) on 1 May 2007 in the Haut Glacier d'Arolla basin (45°59′31″N, 7°29′41″E; Swiss Coordinate System CH1903+ latitude 89000–94000, longitude 604500–609000), estimated from high-resolution digital elevation models. A, B, and C indicate examples of glacierized areas with increased snow depth. Black lines show the glacier boundaries. AWS1, AWS2, and AWS3 are automatic weather stations with indicated frequency distribution for wind direction during the 2006–2007 winter season.

snow drift. The process of preferential deposition does not require high wind speeds, since no snow has to be lifted off the ground and the wind does not have to overcome the friction of the snow on the ground, but acts only with or against the weight of the falling snow.

[5] GPR measurements have been successfully used to estimate snow depth along profiles [e.g., *Jaedicke and Sandvik*, 2002; *Machguth et al.*, 2006] in alpine topography, but to our knowledge, there is no area-covering high-resolution data set of snow distribution. Such a data set, in addition to high-resolution modeling of wind, is needed to analyze and quantify the often suggested relationship between local wind fields and snow distribution. In this study, we provide evidence for this relationship by correlating modeled wind fields with fully distributed snow depth measurements for an alpine catchment. Apart from providing new evidence on the previously discussed influence of horizontal wind fields on snow distribution [e.g., *Pomeroy et al.*, 1993; *Liston and Sturm*, 1998; *Jaedicke and Sandvik*, 2002; *King et al.*, 2004; *Jaedicke and Gauer*, 2005; *Mott et al.*, 2008; *Bernhardt et al.*, 2009], we introduce the correlation between vertical wind component and snow distribution, which provides new insight into the process of wind-driven snow distribution. This correlation between snow depth and horizontal as well as vertical wind velocities can be considered for parameterizations of wind-driven snow accumulation processes in order to improve glacier mass balance models. We specifically think that the process of preferential deposition can be parameterized in a simple way as a function of wind speed only, without the requirement to model snow metamorphism, which is required for the description of snow surface properties in snow drift modeling.

[6] Abrupt changes of topography in steep terrain lead to local acceleration of air masses. These vertical and horizontal accelerations also change the pressure field and have a nonlocal influence on the flow field. Therefore, a nonhydrostatic model is required in order to describe wind fields in such terrain. Wind fields were modeled using the atmospheric prediction model called the Advanced Regional Prediction System (ARPS) [*Xue et al.*, 2000, 2001]. Both horizontal and vertical components of the resulting wind fields were analyzed in relation to snow depth estimations, which were obtained using high-resolution light detection and ranging (lidar) digital elevation models (DEMs). The correlation between modeled wind fields, measured snow depth, and glacierization patterns leads us to conclude that wind fields not only determine snow accumulation in mountainous areas but are an important parameter for the mass balance distribution of glaciers and their location. This is crucial for sustainment of small glaciers, which are characterized by increased winter accumulation.

2. Study Site and Measurements

2.1. Study Site

[7] The catchment of the Haut Glacier d'Arolla is located in southwestern Switzerland on the main Alpine divide. It is about 13 km^2, with a glacierized area of 5.3 km^2 (Figure 1, black lines) and an elevation range from 2500 to 3800 m above sea level (asl). The largest glacier in the area is the north facing Haut Glacier d'Arolla (4.4 km^2). The catchment has several smaller cirque glaciers, which occupy an area of 0.9 km^2. The topography is characterized by steep slopes, with 30% of the catchment steeper than 40°.

[8] The distribution of wind directions from automatic weather stations (AWSs) inside the catchment (Figure 1, AWS1 and AWS2) is dominated by wind blowing down the main valley, while the wind distribution measured at a station on a nearby ridge west of the catchment at 3300 m asl (AWS3) shows larger variations of wind direction. The interannual variability in the dominant wind direction at the three AWSs is small. Station AWS3 was assumed to represent the synoptic wind patterns in the region and was used to estimate the prevailing wind directions since it is located on a nearby ridge and is minimally influenced by the local topography.

2.2. High-Resolution DEMs

[9] Two DEMs for the entire basin were generated using a high-resolution helicopter-borne lidar handheld system (Riegl 2-D airborne laser scanner LMS-Q240i-60). (Complete information about the system can be found at www.helimap.ch.) The handheld system allows for the orientation of the sensor toward steep slopes to limit the degradation of accuracy with increasing slope. The spatial resolution of the lidar system was about 4 points m^{-2}, but all data were gridded to a regular 10 m grid using the continuous curvature surface gridding algorithm after *Wessel and Smith* [1998]. The vertical and horizontal accuracy of the lidar

system was 10–15 cm. The DEMs correspond to survey flights on 1 November 2006 and 1 May 2007, at the beginning and the end of the accumulation season, respectively.

3. Methods

3.1. Snow Depth Estimation From DEMs

[10] Winter accumulation over the entire basin (Figure 1) was estimated from relative elevation changes between two DEMs. Because of recent thinning and slowing of the main glacier (A. Hubbard and D. Mair, personal communication, 2007), the ice movement perpendicular to the surface was assumed to have a marginal effect on these snow depth estimations. This assumption was verified with snow depth estimations from DEMs against 100 ground measurements of snow depth, which were conducted on the same day as the spring lidar survey. The correlation coefficient r between measured and estimated snow depth was 0.95, and the root-mean-square deviation, assuming a linear regression with slope equal to 1, was 15 cm. The surface melt before 1 May 2007 was considered too small to affect the estimated snow depth distribution patterns in the larger, upper part of the catchment, which is emphasized in this paper. According to a study by *Huss et al.* [2008], surface melt in the region, for that particular period, significantly affected the lower part of the catchment (below 2700 m asl) and was in the order of the lidar accuracy for elevations above 2700 m asl. The settlement of snow that was present before 1 November was not taken into account. This error was considered negligible since there was little snowfall prior to December 2006 or snow that persisted through the previous summer. Accepting these approximations, these data were ideally suited for exploring the correlation between snow accumulation and wind patterns. Because wind measurements at sufficiently high resolution do not exist, we used modeled wind fields. The largest snow depth was found over glacierized areas (Figure 1), especially over the accumulation area of the main glacier (Figure 1, area C), as well as over the small cirque glaciers (e.g., Figure 1, areas A and B). Avalanche deposits were observed at the foot of steep slopes (e.g., Figure 1, area A) and was restricted to the vicinity of steep walls.

3.2. Wind Field Modeling With ARPS

[11] The mesoscale atmospheric model ARPS was used to model wind fields [*Xue et al.*, 2000, 2001]. Recent studies show that this model can be used for microscale airflow to reproduce characteristic flow features, such as speedup effects at mountain ridges, as well as critical flow features of steep terrain, such as blocking or flow separation [*Jaedicke and Gauer*, 2005; *Chow et al.*, 2006; *Weigel et al.*, 2006; *Mott et al.*, 2008; *Raderschall et al.*, 2008].

[12] In ARPS, the nonhydrostatic compressible Navier-Stokes equations are solved in a 3-D domain. The conservation equations for momentum, heat, mass, states of water (vapor, liquid, and ice), and the equation of the state of moist air are considered. A comprehensive description of the ARPS model is given by *Xue et al.* [2000, 2001].

[13] For this study, a horizontal grid spacing of 30 m was found to be sufficient to reproduce the main flow characteristics of the catchment. The vertical grid spacing varied between about 3 m near the ground and 100 m in the upper layers. For our discussion, we only considered the first layer above the ground at about 3 m. The vertical extent of the model domain was 3000 m.

[14] The flow model was initialized with different atmospheric profiles for the three most frequent wind directions measured at the station AWS3 during the period between the two lidar surveys: 30°, 120°, and 235° (Figure 1, wind rose of AWS3). The vertical profiles of the atmospheric boundary layer (ABL) were assumed to be slightly stable stratified (-6.5 K km^{-1}); the depth of the ABL was set to 500 m. Above the ABL the atmosphere was defined as neutral. A humid atmosphere of 95% relative humidity was assumed since we were interested in the wind influence on snow distribution during precipitation events. The initial wind profile was assumed to be logarithmic within the atmospheric boundary layer and constant (13 m s^{-1}) above. An aerodynamic roughness length of 0.01 m for snow-covered alpine topography was chosen over the entire domain. Each model run started from a horizontally homogeneous base state.

[15] The flow fields for this study were calculated for a rather short integration time of 30 s, after which the initial adaptation of the flow field to the topography was established and the mean flow features were found to be well developed. After a longer integration time, turbulent flow structures dominated the flow field characteristics and an averaging operation would be required to obtain the mean flow [*Lehning et al.*, 2008; *Raderschall et al.*, 2008].

[16] In order to maintain model stability, which is not given for slopes steeper than 50°, the topography was smoothed using a low-pass filter (20 × 20 kernels, with all kernel array elements weighted equally). The smoothing did not affect the location of main ridges, valleys, and troughs, which are important for local wind fields.

4. Results and Discussion

[17] The measured two predominant but opposite wind directions in the main valley (Figure 1, AWS1 and AWS2) can be attributed to channel effects, which were reproduced by ARPS, as well as to katabatic winds, which are not captured by the model. The modeled wind directions of the three prevailing wind fields (Figures 2a, 2d, and 2g) agreed well with the measured wind directions inside the catchment (Figure 3), which are strongly influenced by topography. However, the large-scale flow is not deflected all the way toward the local glacier downslope, as observed, which is probably due to the lack of katabatic flow in the model. The comparison of mean measured wind directions and the three modeled wind directions show that the modeled flow gets diverted by the steep slopes from the initial direction toward the measured direction at AWS1 and AWS2. The effect of dominating features like depressions and smaller ridges was clearly captured in the simulations despite topographic smoothing (Figures 2 and 4).

[18] As expected, because of speedup effects, the horizontal wind velocity was highest over ridges and peaks, while it was lowest over flat areas (Figures 2b, 2e, and 2h), which are mostly glacierized. The vertical wind component was strongly dependent on wind direction (Figures 2c, 2f, and 2i), positive on the windward side and negative on the lee side of a ridge. This can be illustrated in the following example: when using 235° as initial wind direction, the small

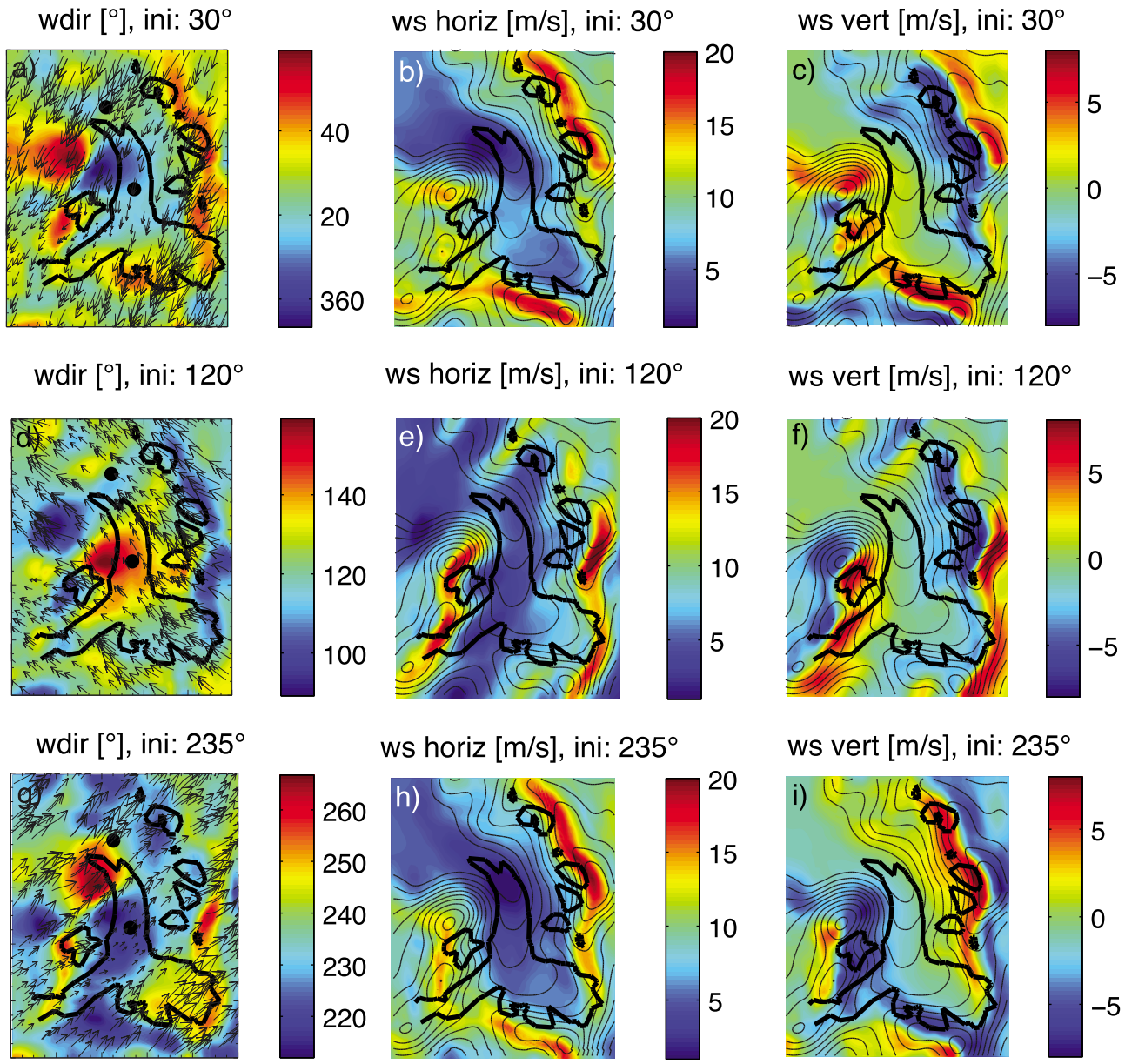

Figure 2. (a, d, g) Simulated wind direction, (b, e, h) horizontal wind velocity, and (c, f, i) vertical wind velocity (positive upward) of the three prevailing wind fields in the region. The topography used for the simulations is shown with the overlaid contours. Black dots indicate the locations of automatic weather stations AWS1 and AWS2. Thick black lines define glacierized areas.

glaciers east of the main valley (e.g., Figure 1, area B) were in the windward side of a ridge and experienced upward wind, while the glacier west of the main valley (Figure 1, area A) was in the lee side of a ridge and experienced downward winds, which led to increased deposition. If initiated with 30°, the glaciers east and west of the main valley showed opposite behavior than when initiated from 235°. This effect was most pronounced over small cirque glaciers close to steep slopes. Additionally, we also calculated the wind velocity normal to the local topography (Figure 4), which would be zero in a nondivergent flow field. The surface-normal velocity should be a direct measure of increased or decreased local erosion and deposition from suspension and preferential deposition [*Lehning et al.*, 2008]. These normal velocities show less uniform patterns for the same side of a ridge as the vertical wind components in Figures 2c, 2f, and 2i and highlight the curvature (convexity or concavity) of smaller surface features. Concave features show, in general, lower (less positive) wind speed than convex features, which means that they experience fewer updrafts and less erosion and therefore higher deposition velocities of snow and higher accumulation. In general, Figure 4 shows similar patterns to the vertical wind velocity in Figure 2 for wind directions 30° and 235°, with the exceptions of some smaller regions (e.g., Figures 4a and 4c, dashed circles), which show a different behavior reflecting small-scale features of topography. For the 120° wind direction, the region which shows a different behavior than

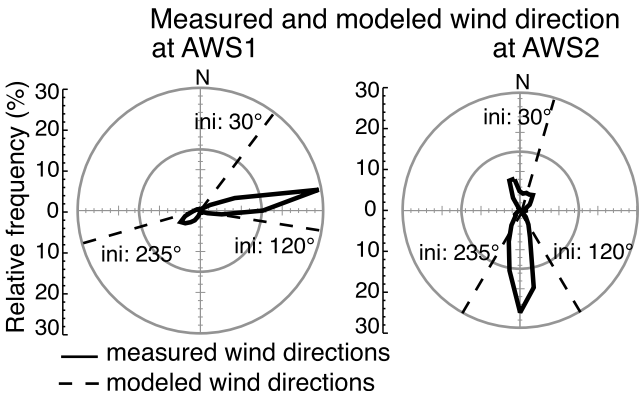

Figure 3. Frequency distribution of wind directions at automatic weather stations (left) AWS1 and (right) AWS2 compared to the three modeled wind directions at the same locations (dashed lines).

the vertical wind component (Figure 2f) is somewhat larger (Figure 4b, dashed circles) but can also be attributed to small-scale terrain features. The dissimilar behavior of the vertical wind speed and the surface-normal wind velocity can be explained by separating the numerical effects of the slope gradient from the physical effects which are purely caused by the modification of the airflow by local topographical features.

[19] Snow distribution in steep alpine terrain is determined by wind and avalanches. Wind leads either to erosion and deposition of already deposited snow, which is known as snow drift, or to preferential deposition of precipitation. While snow drift is dependent not only on winds but also on snow surface properties [e.g., *Pomeroy*, 1988; *Liston and Sturm*, 1998; *Clifton and Lehning*, 2008], preferential deposition is mainly governed by winds. *Lehning et al.* [2008] explain preferential deposition as the spatially varying deposition of precipitation due to the topography-induced flow field modification close to the surface. Higher wind speeds and updrafts in the windward side of a mountain ridge cause reduced deposition velocities, which means that the vertical wind speed is positive (showing upward). A decreased deposition velocity on the windward side further leads to increased snow accumulation in an air parcel that travels uphill toward the crest. As soon as the air parcel crosses the ridge, it enters an area of decreased mean wind velocity with higher deposition velocity (influenced by the vertical velocity), and the air parcel additionally has the increased snow concentration [*Lehning et al.*, 2008]. According to *Lehning et al.* [2008, paragraph 29], "these are two effects that cause uneven snow distribution in complex terrain during snowfall in the absence of local erosion." Since preferential deposition of snow is linked to precipitation events, when relative humidity is near saturation, we do not discuss sublimation.

[20] In order to directly correlate the effect of wind velocities with the seasonal snow depth distribution, the three modeled wind fields were averaged for the observation period, using weighting factors for each wind field. The weighting factors were calculated from measured wind directions at AWS3 during recorded precipitation events at AWS1 and therefore account for predominant wind directions during precipitation events. The total measured precipitation is divided into precipitation coming from different direction ranges, which are represented by the three modeled wind fields. The winter precipitation between 1 November 2006 and 1 May 2007 was 380 mm. The precipitation concurrent with southwestern winds (measured range, 180°–290°; modeled, 235°) was the largest with 230 mm (weighting factor 0.61); southeastern winds (measured range, 90°–180°; modeled, 120°) had precipitation measuring 85 mm (weighting factor 0.22); and northern winds (measured range, 290°–90°; modeled, 30°) had precipitation measuring 65 mm (weighting factor 0.17). The mean seasonal wind velocity *ws* for each component was then calculated using these weighting factors:

$$ws = 0.17ws_{30} + 0.22ws_{120} + 0.61ws_{235}, \quad (1)$$

where ws_{120} is the wind velocity when the model is initiated from 120°, ws_{235} is the wind velocity when the model is initiated from 235°, and ws_{30} is the wind velocity when the

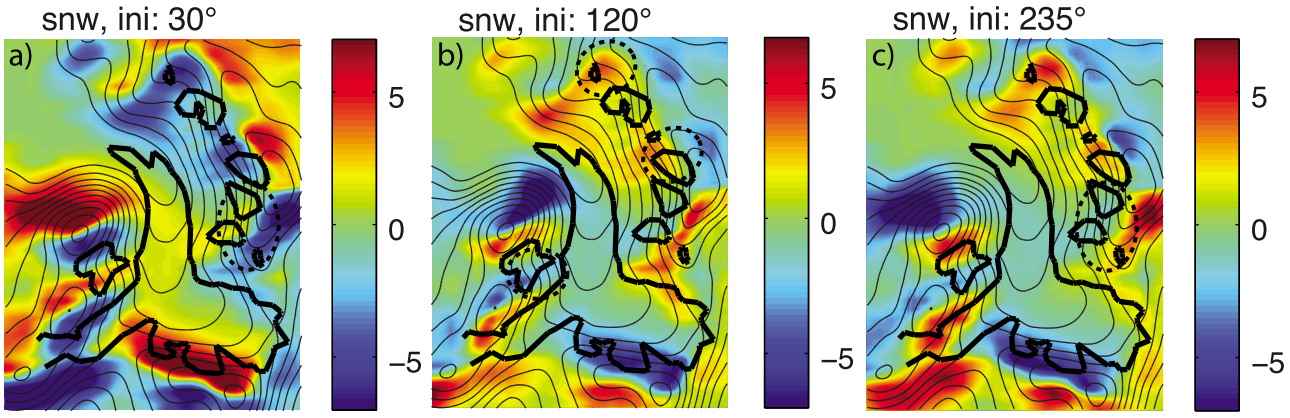

Figure 4. (a, b, c) Surface-normal wind velocity of the three prevailing wind fields in the region. The topography used for the simulations is shown with the overlaid contours. Thick black lines define glacierized areas. (Note that for Figure 4, we suppressed values which were exceeding ±7 m s^{-1} for easier comparison with vertical velocities in Figure 2.)

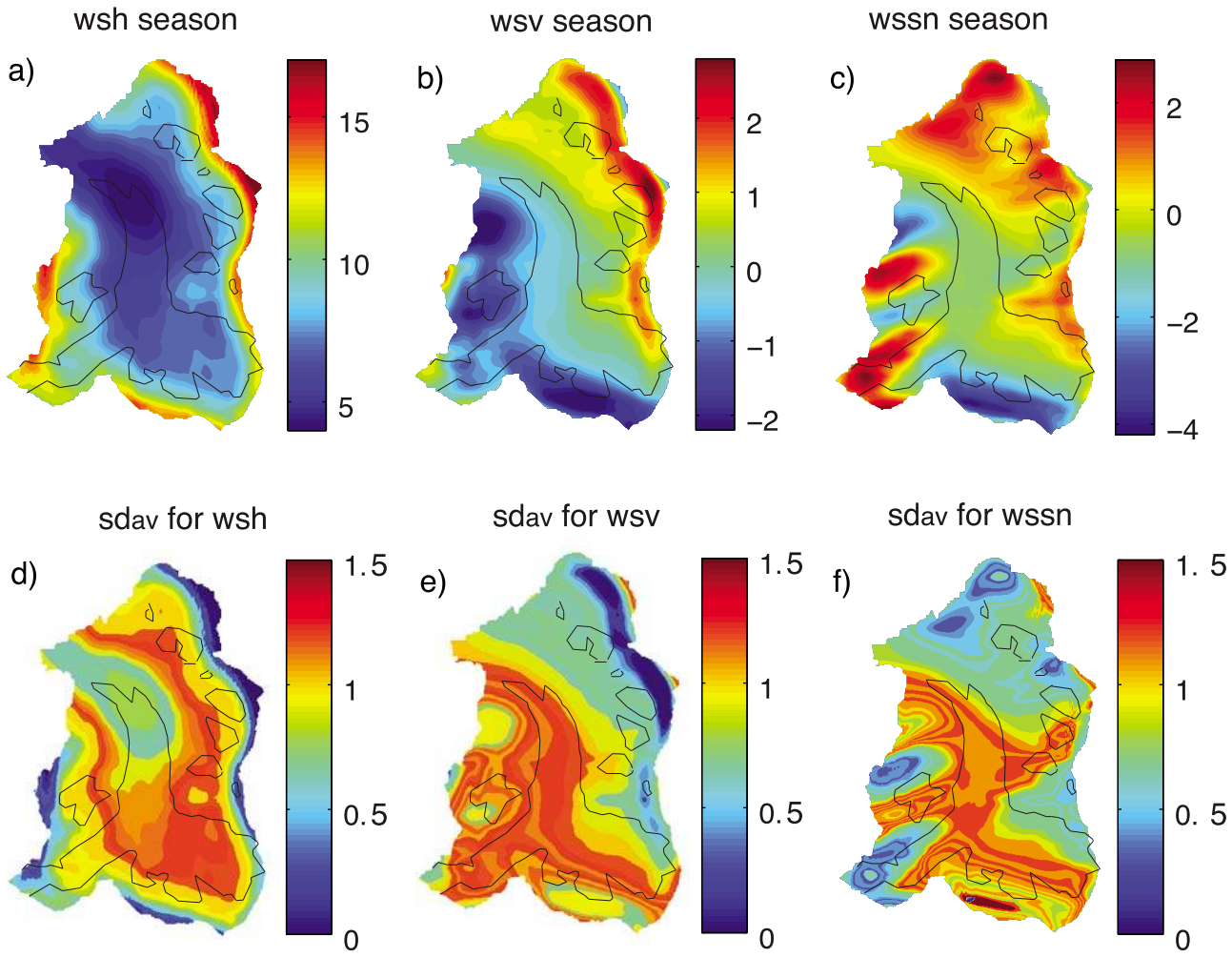

Figure 5. Seasonally averaged (a) horizontal, (b) vertical, and (c) surface-normal wind velocity (weighted by the precipitation amount for the observation period and averaged over cells within a certain wind velocity increment) and (d, e, f) lidar-estimated snow depth averaged over same cells as the different wind speed components above. The black lines indicate glacier boundaries.

model is initiated from 30°. The weighting can be applied to all considered wind velocities (vertical, horizontal, or surface normal) in the same way. These seasonally averaged wind velocities are not highly sensitive to the weighting factors, as long as we assume the winds from the southwestern quadrant to be the most frequent, as they are in the observed frequency distribution of wind directions from AWS3 in Figure 1. In order to obtain the general pattern of the snow depth distribution, and to correlate those to wind velocities, the wind speeds as well as the snow depths were averaged over cells within a certain wind velocity increment. The increments for horizontal wind velocity were 0.5 m s^{-1} and for vertical and surface-normal wind velocity were 0.2 m s^{-1}. The increments were chosen to obtain approximately the same number of averaged points for each wind component. Figure 5 shows these seasonally averaged horizontal (Figure 5a), vertical (Figure 5b), and surface-normal (Figure 5c) wind velocities inside the catchment (weighted by the wind-related precipitation amount for the observation period and averaged over cells within a certain wind velocity increment) and shows lidar-estimated snow depth (Figures 5d, 5e, and 5f) averaged over the same cells as the different wind speed components above. Figure 5 shows that regions with lower or negative wind velocities correspond to larger snow depths. The scatterplots of the averaged wind speeds for a certain increment (Figures 5a, 5b, and 5c) against the averaged snow depths over the same cells (Figures 5d, 5e, and 5f) show that the resulting seasonal horizontal wind velocity was negatively correlated with snow depth above 6 m s^{-1} (Figure 6a) and indicate that there was less snow for higher horizontal wind velocities. The points for wind speeds below 6 m s^{-1} were mainly from the proglacial area below 2700 m asl, which had already experienced melt at the time of the second lidar survey, as discussed in section 3. This is also illustrated in Figure 5d, where the averaged snow depth over the lower part of the glacier tongue and the proglacial area have less snow than the rest of the main glacier. The resulting seasonal vertical wind velocity, as well as the surface-normal velocity, also showed a negative correlation with snow depth (Figures 6b and 6c), indicating more snow with increasing negative velocity values. While the horizontal velocity can

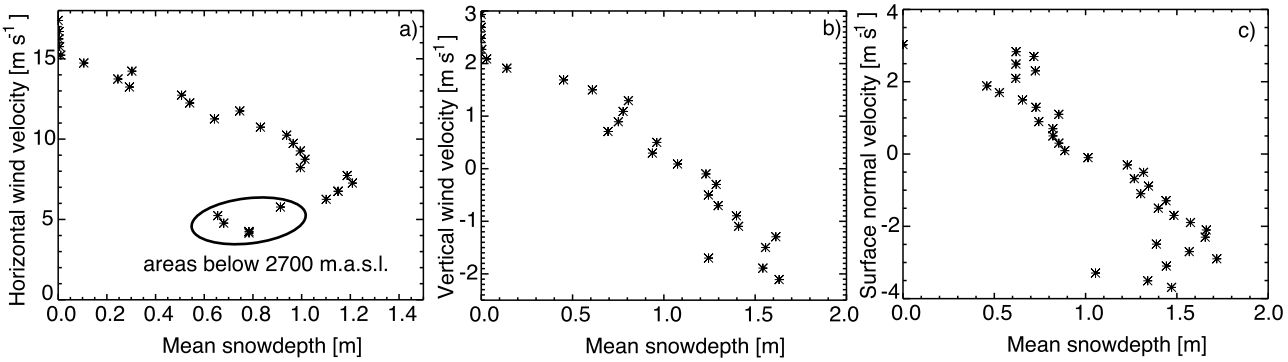

Figure 6. Seasonally averaged (a) horizontal, (b) vertical, and (c) surface-normal wind velocity (weighted by the precipitation amount for the observation period and averaged over cells within a certain wind velocity increment) against snow depth (averaged over the same cells as the different wind speed components).

be the same in the windward and the lee side of a ridge, the vertical and surface-normal velocities are either positive or negative, depending on the wind direction, and are therefore also an indirect measure of the wind direction. This makes them relevant for understanding processes that govern wind-driven snow accumulation (e.g., on either side of a ridge).

[21] The strongest negative vertical velocities often occurred directly behind ridges, which are often characterized by steep slopes and are likely to be affected by avalanches. This could account for some of the discrepancies between the seasonally averaged wind speed and the corresponding averages of snow depth, as, for example, on the steep wall at the southern boundary of the main glacier (Figures 5e and 5f). However, avalanches in very steep areas are likely to have a short reach (e.g., Figure 1, area A) and therefore only affect a small area. The reason for the short reach is that steep slopes never accumulate large snow masses, which would result in large avalanches with a further reach [*Lied and Toppe*, 1989; *Sovilla et al.*, 2006]. Above mean horizontal velocities of 15 m s^{-1}, mean vertical velocities of 2 m s^{-1}, and mean surface-normal velocities of 3 m s^{-1}, there was no significant snow accumulation. The correlation between wind velocity and snow depth points to a strong wind influence on snow accumulation and glacierization patterns.

5. Summary and Conclusions

[22] The goal of this study was to verify the often suggested relationship between local wind fields and snow accumulation. We did this by comparing modeled wind fields with snow depth estimations from high-resolution lidar DEMs in a glacierized alpine catchment. Snow depth distribution was not only compared to horizontal wind components, but we also discussed the influence of the vertical wind component and the surface-normal wind component on snow depth distribution, which, to our knowledge, has not been done previously. It is a novel contribution of this work that we achieve a reasonable correlation between wind fields and observed snow distribution despite the simplifications in our analysis.

[23] Our results showed increased horizontal wind velocity over ridges and along steep slopes and reduced horizontal wind velocity over flat and glacierized areas with the highest accumulation. The vertical wind velocity and the surface-normal velocity, which determine the settling velocity of snow during precipitation or snow drift events, was strongly dependent on the wind direction, with especially high values (positive or negative) in troughs close to steep slopes where small cirque glaciers occur. Depending on the wind direction, these areas experienced either updrafts leading to erosion and reduced deposition on the windward side of mountain ridges or downward winds leading to increased deposition in the lee of mountain ridges. We observed a clear negative correlation between seasonally averaged horizontal and vertical wind velocities and snow depth. This observation is not only relevant for the existence of small glaciers, for whose mass balance winter accumulation plays an important role, but also shows that wind fields govern snow distribution patterns in the entire catchment. Local wind fields can also affect the energy balance over snow and ice because reduced wind speed over flat areas is likely to lead to smaller turbulent fluxes. The reduction in turbulent fluxes results in reduced melt and sublimation of snow and ice. This effect was not quantified in this study but should be addressed in the future in order to better understand the energy balance over snow and ice.

[24] Our results emphasize the relationship between local wind fields, snow accumulation, and glacierized areas. We believe that accurate modeling of wind fields is a key factor for understanding the mass balance of glaciers in mountainous areas. Snow erosion and subsequent deposition of already deposited snow (snow drift), as well as spatially varying preferential deposition of snowfall, are caused by topography-induced flow field modification close to the surface. While the relevance of snow drift has been often discussed in past literature [e.g., *Mellor*, 1965; *Radok*, 1977; *Pomeroy*, 1988; *Liston and Sturm*, 1998; *Clifton and Lehning*, 2008], we want to emphasize the preferential deposition of precipitation. *Lehning et al.* [2008] suggest that updrafts in the windward side of a mountain ridge cause reduced deposition, while downward winds in the lee of ridges cause increased deposition. The observed correlation between snow accumulation and wind velocities, without considering snow surface properties, along with the analysis by *Lehning et al.* [2008], makes it likely that the preferential

deposition of precipitation is one of the dominant processes for snow distribution in alpine areas at the basin scale. This correlation can be used for parameterizations of preferential deposition in order to improve glacier mass balance models. Since preferential deposition is mainly governed by winds and does not require the knowledge of snow surface properties, it can be parameterized in a simpler way than snow drift and could be used in most mass balance models, without the requirement for modeling snow metamorphism.

[25] **Acknowledgments.** We thank A. Aschwanden, A. Beeli, F. Faure, M.G. Haas, H. Horgan, M. Huss, C. Marti, P. Perona, S. Rimkus, M. Schneebeli, J. Schweizer, C. Senn, and J. Vallet for their valuable contributions. Parts of the ARPS simulations have been made with support from the Swiss National Supercomputing Centre, CSCS. The study was carried out with support from the Swiss National Science Foundation.

References

Bernhardt, M., G. Zangl, G. E. Liston, U. Strasser, and W. Mauser (2009), Using wind fields from a high-resolution atmospheric model for simulating snow dynamics in mountainous terrain, *Hydrol. Processes*, *23*, 1064–1075.

Chow, F. K., A. P. Weigel, R. L. Street, M. W. Rotach, and M. Xue (2006), High-resolution large-eddy simulations of flow in a steep alpine valley. Part I: Methodology, verification, and sensitivity experiments, *J. Appl. Meteorol.*, *45*(1), 63–86.

Clifton, A., and M. Lehning (2008), Improvement and validation of a snow saltation model using wind tunnel measurements, *Earth Surf. Processes Landforms*, *33*(14), 2156–2173.

Föhn, P. M. B., and R. Meister (1983), Distribution of snow drifts on ridge slopes: Measurements and theoretical approximations, *Ann. Glaciol.*, *4*, 52–57.

Gauer, P. (2001), Numerical modeling of blowing and drifting snow in alpine terrain, *J. Glaciol.*, *47*, 97–110.

Gray, D. M., and D. H. Male (Eds.) (1981), *Handbook of Snow: Principles, Processes, Management and Use*, Pergamon, Oxford, U. K.

Hoffmann, M. J., A. G. Fountain, and J. M. Achuff (2007), 20th-century variations in area of cirque glaciers and glacierets, Rocky Mountain National Park, Rocky Mountains, Colorado, USA, *Ann. Glaciol.*, *46*, 349–354.

Huss, M., A. Bauder, and M. Funk (2008), Homogenization of long term mass balance time series, *Ann. Glaciol.*, *50*, 198–206.

Jaedicke, C., and P. Gauer (2005), The infuence of drifting snow on the location of glaciers on western Spitzbergen, Svalbard, *Ann. Glaciol.*, *42*, 237–242.

Jaedicke, C., and A. D. Sandvik (2002), High resolution snow distribution data from complex arctic terrain: A tool for model validation, *Nat. Hazards Earth Syst. Sci.*, *2*, 147–155.

King, J. C., P. S. Anderson, D. G. Vaughan, G. W. Mann, S. D. Mobbs, and S. B. Vosper (2004), Wind-borne redistribution of snow across an Antarctic rise, *J. Geophys. Res.*, *109*, D11104, doi:10.1029/2003JD004361.

Kuhn, M. (1995), The mass balance of very small glaciers, *Z. Glestcherkd. Glazialgeol.*, *31*, 171–179.

Kuhn, M. (2003), Redistribution of snow and glacier mass balance from a hydrometeorlological model, *J. Hydrol.*, *282*, 95–103.

Lehning, M., H. Löwe, M. Ryser, and N. Raderschall (2008), Inhomogenious precipitation distribution and snow transport in steep terrain, *Water Resour. Res.*, *44*, W07404, doi:10.1029/2007WR006545.

Lied, K., and R. Toppe (1989), Calculation of maximum snow-avalanche run-out distance by use of digital terrain models, *Ann. Glaciol.*, *13*, 164–169.

Liston, G. E., and M. Sturm (1998), A snow-transport model for complex terrain, *J. Glaciol.*, *44*, 498–516.

Machguth, H., O. Eisen, F. Paul, and M. Hoelzle (2006), Strong spatial variability of snow accumulation with helicopter-borne GPR on two adjacent alpine glaciers, *Geophys. Res. Lett.*, *33*, L13503, doi:10.1029/2006GL026576.

Mellor, M. (1965), Blowing snow, *Monogr. III-A3c*, U.S. Army Cold Reg. Res. Eng. Lab., Hanover, N. H.

Mott, R., F. Faure, M. Lehning, H. Löwe, B. Hynek, G. Michlmayr, A. Prokop, and W. Schöner (2008), Simulation of seasonal snow-cover distribution for glacierized sites on Sonnblick, Austria, with the Alpine3D model, *Ann. Glaciol.*, *49*, 155–160.

Pomeroy, J. W. (1988), Wind transport of snow, Ph.D. thesis, 226 pp., Div. of Hydrol., Univ. of Sask., Saskatoon, Sask., Canada.

Pomeroy, J. W., D. M. Gray, and P. G. Landine (1993), The Prairie Blowing Snow Model: Characteristics, validation, operation, *J. Hydrol.*, *144*, 164–192.

Raderschall, N., M. Lehning, and C. Schaer (2008), Fine-scale modeling of the boundary layer wind field over steep topography, *Water Resour. Res.*, *44*, W09425, doi:10.1029/2007WR006544.

Radok, U. (1977), Snow drift, *J. Glaciol.*, *19*, 123–139.

Sovilla, B., P. Burlando, and P. B. Bartelt (2006), Field experiments and numerical modeling of mass entrainment in snow avalanches, *J. Geophys. Res.*, *111*, F03007, doi:10.1029/2005JF000391.

Weigel, A. P., F. K. Chow, M. W. Rotach, R. L. Street, and M. Xue (2006), High-resolution large eddy simulations of flow in steep alpine valley. Part II: Flow structure and heat budgets, *J. Appl. Meteorol.*, *45*(1), 87–107.

Wessel, P., and W. H. F. Smith (1998), New, improved version of the generic mapping tools released, *EOS Trans. AGU*, *79*(47), 579.

Winstral, A., and D. Marks (2002), Simulating wind fields and snow redistribution using terrain-based parameters to model snow accumulation and melt over a semi-arid mountain catchment, *Hydrol. Processes*, *16*, 3605–3626.

Winstral, A., K. Elder, and R. E. Davis (2002), Spatial snow modeling of wind-redistributed snow using terrain based parameters, *J. Hydrometeorol.*, *3*, 524–537.

Xue, M., K. K. Droegemeier, and V. Wong (2000), The Advanced Regional Prediction System (ARPS)—A multi-scale nonhydrostatic atmospheric simulation and prediction model. Part I: Model dynamics and verification, *Meteorol. Atmos. Phys.*, *75*, 161–193.

Xue, M., K. K. Droegemeier, V. Wong, A. Shapiro, K. Brewster, F. Carr, D. Weber, Y. Liu, and D. Wang (2001), The Advanced Regional Prediction System (ARPS)—A multi-scale nonhydrostatic atmospheric simulation and prediction model. Part II: Model physics and applications, *Meteorol. Atmos. Phys.*, *76*, 143–165.

P. Burlando, Institute of Environmental Engineering, ETH Zurich, HIL D22.3, Zurich CH-8093 Switzerland. (burlando@ifu.baug.ethz.ch)

R. Dadic, Department of Atmospheric Sciences, University of Washington, Seattle, WA 98195-1640, USA. (dadic@atmos.washington.edu)

M. Lehning and R. Mott, WSL Institute for Snow and Avalanche Research SLF, Flüelastr. 11, Davos CH-7260, Switzerland. (lehning@slf.ch; mott@slf.ch)